Exact calculation of the second-order Born terms for exotic-atom formation into excited states

Akinori Igarashi, Nobuyuki Toshima, and Takeshi Ishihara
Institute of Applied Physics, University of Tsukuba, Tsukuba, Ibaraki 305, Japan
(Received 19 May 1992)

Differential cross sections of the second-order Born approximation are calculated exactly for particle transfer to $1s$, $2s$, and $2p$ states of exotic atoms. The processes can be classified into three types. In the collision of $p+(p\mu^-)$, the Thomas process [Proc. R. Soc. London **114**, 561 (1927)] takes place only via a single path as in the proton-hydrogen case, while, in the collision of $\mu^+ + (p\mu^-)$, it can proceed via two paths that interfere destructively or constructively depending on the parity of the final state as in the positronium formation from a hydrogen atom. In the third type, in which all the three particles have an equal mass as in positron-positronium collisions, the critical angle occurs at 180° only and the two second-order terms which are forbidden in classical mechanics are contributing significantly to the backscattering.

PACS number(s): 34.70.+e, 36.10.Dr

I. INTRODUCTION

The Thomas double-scattering mechanism [1] has been one of the most controversial problems in the field of atomic collisions since Drisko [2] established the connection between this classical mechanism and the second-order Born terms in the quantum-mechanical description. In the original picture of Thomas, two successive binary collisions lead to electron capture by an incident ion from a target atom. Though the Thomas mechanism is essentially a second-order process, it tends to dominate the first-order contribution as the collision energy increases [3]. This mechanism plays an important role not only in electron capture but also in many types of rearrangement collisions, e.g., positronium formation [4] and atom transfer in chemical reactions [5]. A particular scattering angle, which is called the Thomas critical angle, is favored for the projectile and one of the target particles to move off together after the two binary collisions. This angle is determined by the conservation requirements of the total momentum and energy in the classical mechanics. The differential cross sections show a prominent peak there. In the quantal description, the Thomas mechanism manifests itself as a singularity of the Green's function in the second-order Born terms. The angle determined by the singularity coincides with the classical prediction [6].

In general three-body rearrangement collisions,

$$P+(Tc)\rightarrow(Pc)+T\ , \tag{1}$$

where the particles in a bracket denotes a bound state, three ways of Thomas mechanism are possible: (i) P hits c in the first binary collision and c makes the second collision with T. (ii) P hits c in the first collision and the recoiled P makes the second collision with T. (iii) P hits T in the first collision and the ejected T makes the second collision with c. The process (i) is important for electron capture in ion-atom collisions. The critical angle in the center-of-mass frame for (i) is given by [6]

$$\cos\theta_C=\frac{3\nu_T\nu_P-1}{2(\nu_T\nu_P)^{3/2}}\quad \text{for } \tfrac{1}{4}\le\nu_T\nu_P\le 1\ , \tag{2}$$

with

$$\nu_P=\frac{M_P}{M_P+M_c} \tag{3}$$

and

$$\nu_T=\frac{M_T}{M_T+M_c}\ , \tag{4}$$

where M's are the masses of the labeled particles. This scattering angle is generally very small for ion-atom collisions and it amounts to 0.94 mrad for proton-hydrogen collisions. The critical angle for (ii) is given by

$$\cos\theta_C=\frac{1}{2\sqrt{\nu_T\nu_P}}\left[1+\nu_T\nu_P-\frac{\nu_P(1-\nu_T\nu_P)^2}{\nu_T(1-\nu_P)^2}\right]$$
$$\text{for } \nu_P\le\nu_T\le\frac{\nu_P}{(1-2\nu_P)^2}\ . \tag{5}$$

The critical angle of the process (iii) is obtained with ν_T and ν_P interchanged in Eq. (5).

Exact calculations of the second-order Born amplitudes for electron capture have been reported in several papers [7–9]. However, all of the performed calculations are only for capture into the $1s$ state and the contribution of capture into excited states is generally taken into account by multiplying a factor of 1.2 under the assumption that the same scaling law of $1/n^3$ (n is the principal quantum number of the final state) holds as the high-energy behavior of the Oppenheimer-Brinkmann-Kramers approximation [10]. Although Shakeshaft and Spruch [11] showed that the *classical* double-scattering cross section satisfies the same scaling law in the high-energy limit, it is not evident whether purely quantal, especially differential, cross sections also satisfy the same scaling law.

 ©1992 The American Physical Society

Recently, the second-order Born cross sections for positronium formation into excited states have been calculated accurately [12]. In this process, the two paths of (i) and (ii) give the same Thomas critical angle of 45°. These two amplitudes interfere destructively for capture into states with even parity and constructively for capture into states with odd parity [4]. Loss of significant figures is serious owing to cancellation error when destructive interference takes place. Highly accurate calculation of scattering amplitudes is required for reliable analysis of the interference effect.

In this article, we calculate the second-order Born cross sections for rearrangement collisions involving exotic atoms. The first- and second-order scattering amplitudes for transfer to the shell of $n=1$ or 2 are calculated exactly. Atomic units are used unless otherwise stated.

II. FORMULATION

We calculate the cross sections of the second-order Born approximation for the rearrangement collision (1). The initial and the final three-body wave functions are composed of an atomic bound state and a plane wave representing the relative motion between the projectile and the target:

$$\Phi_i=\phi_i(\mathbf{r}_T)\exp(i\mathbf{k}_i\cdot\mathbf{R}_T)\ , \tag{6}$$

$$\Phi_f=\phi_f(\mathbf{r}_P)\exp(i\mathbf{k}_f\cdot\mathbf{R}_P)\ , \tag{7}$$

where $\mathbf{r}_T$ ($\mathbf{r}_P$) is the position vector of the particle c measured from the particle T (P) and $\mathbf{R}_T$ ($\mathbf{R}_P$) is the position vector of the particle P [the center of mass of the atom (Pc)] measured from the center of mass of the atom (Tc) (the particle T). $\mathbf{k}_i$ and $\mathbf{k}_f$ are the wave vectors of the relative motion in the initial and the final channels. The first- and second-order terms of the T matrix elements are

$$T_1=\langle\Phi_f|V_f|\Phi_i\rangle \tag{8}$$

and

$$T_2=\langle\Phi_f|V_fG_0^+V_i|\Phi_i\rangle\ , \tag{9}$$

where V_i is the interaction between the projectile and the target atom in the entrance channel and V_f its counterpart in the exit channel:

$$V_i=\frac{Z_PZ_c}{r_P}+\frac{Z_PZ_T}{R}\ , \tag{10}$$

$$V_f=\frac{Z_TZ_c}{r_T}+\frac{Z_PZ_T}{R}\ . \tag{11}$$

R is the distance between the particles P and T, and Z's are the charges of the labeled particle. G_0^+ is the free Green's function of the three particles satisfying the outgoing boundary condition:

$$G_0^+=\frac{1}{E-H_0+i\eta}\ . \tag{12}$$

H_0 is the Hamiltonian for three free particles and η is an infinitesimal positive number [13].

The first-order terms are calculated by an analytic procedure [14]. The four terms of the second-order T matrix element are Fourier-transformed to

$$\left\langle\phi_f\left|\frac{1}{r_T}G_0^+\frac{1}{r_P}\right|\phi_i\right\rangle=-\frac{1}{2\pi^4}\int d\mathbf{k}_1\frac{1}{k_1^2}\tilde{\phi}_i(\mathbf{k}_1+\mathbf{B})\times\int d\mathbf{k}_2\frac{1}{k_2^2}\tilde{\phi}_f^*(\mathbf{A}-\mathbf{k}_2)\frac{\nu_PM_c}{k_2^2+2(\nu_P\mathbf{k}_1-\mathbf{A})\cdot\mathbf{k}_2+\frac{\nu_P}{\nu_T}(\mathbf{k}_1+\mathbf{B})^2-2\nu_PM_c\epsilon_i-i\eta}\ , \tag{13}$$

$$\left\langle\phi_f\left|\frac{1}{r_T}G_0^+\frac{1}{R}\right|\phi_i\right\rangle=-\frac{1}{2\pi^4}\int d\mathbf{k}_1\frac{1}{k_1^2}\tilde{\phi}_i(\mathbf{A}-\mathbf{k}_1)\times\int d\mathbf{k}_2\frac{1}{k_2^2}\tilde{\phi}_f^*(\mathbf{k}_1+\mathbf{k}_2+\mathbf{B})\frac{\nu_TM_c}{k_2^2+2(\nu_T\mathbf{k}_1+\mathbf{B})\cdot\mathbf{k}_2+\frac{\nu_T}{\nu_P}(\mathbf{k}_1-\mathbf{A})^2-2\nu_TM_c\epsilon_f-i\eta}\ , \tag{14}$$

$$\left\langle\phi_f\left|\frac{1}{R}G_0^+\frac{1}{r_P}\right|\phi_i\right\rangle=-\frac{1}{2\pi^4}\int d\mathbf{k}_1\frac{1}{k_1^2}\tilde{\phi}_i(\mathbf{k}_1+\mathbf{B})\times\int d\mathbf{k}_2\frac{1}{k_2^2}\tilde{\phi}_f^*(\mathbf{A}-\mathbf{k}_1-\mathbf{k}_2)\frac{\nu_PM_c}{k_2^2+2(\nu_P\mathbf{k}_1-\mathbf{A})\cdot\mathbf{k}_2+\frac{\nu_P}{\nu_T}(\mathbf{k}_1+\mathbf{B})^2-2\nu_PM_c\epsilon_i-i\eta}\ , \tag{15}$$

and

$$\left\langle \phi_f \left| \frac{1}{R} G_0^+ \frac{1}{R} \right| \phi_i \right\rangle = -\frac{1}{2\pi^4} \int d\mathbf{k}_1 \tilde{\phi}_i(\mathbf{k}_1+\mathbf{B}) \tilde{\phi}_f^*(\mathbf{A}-\mathbf{k}_1) \times \int d\mathbf{k}_2 \frac{1}{k_2^2} \frac{1}{|\mathbf{k}_1-\mathbf{k}_2|^2} \frac{\mu}{k_2^2+2\mu\left[\frac{\mathbf{k}_i}{M_P}+\frac{\mathbf{k}_f}{M_T}-\frac{\mathbf{k}_1}{M_P}\right]\cdot\mathbf{k}_2+\frac{\mu}{M_P}(\mathbf{k}_1-\mathbf{A})^2-2\mu\epsilon_f-i\eta} . \tag{16}$$

ϵ_i and ϵ_f are the eigenenergies of the initial and the final bound states, respectively, and $\tilde{\phi}_{i,f}$ are the Fourier transforms of the atomic wave functions:

$$\tilde{\phi}_{i,f}(\mathbf{p}) = \int \phi_{i,f} \exp(-i\mathbf{p}\cdot\mathbf{r}) d\mathbf{r} . \tag{17}$$

The reduced masses and the vectors **A** and **B** are defined as

$$\mu_T = \frac{M_P(M_T+M_c)}{M_P+M_T+M_c} , \tag{18}$$

$$\mu_P = \frac{M_T(M_P+M_c)}{M_P+M_T+M_c} , \tag{19}$$

$$\mu = \frac{M_P M_T}{M_P+M_T} , \tag{20}$$

$$\mathbf{A} = \mathbf{k}_i - \nu_P \mathbf{k}_f , \tag{21}$$

and

$$\mathbf{B} = \mathbf{k}_f - \nu_T \mathbf{k}_i . \tag{22}$$

The four second-order terms (13)–(16) are reduced to three-dimensional integrals utilizing the formula [15]

$$\int d\mathbf{k} \frac{1}{k^2(|\mathbf{k}-\mathbf{k}_1|^2+\lambda_1^2)(|\mathbf{k}-\mathbf{k}_2|^2+\lambda_2^2)} = \frac{\pi^2}{D} \ln\left[\frac{C+D}{C-D}\right] , \tag{23}$$

with

$$C = \lambda_2(k_1^2+\lambda_1^2)+\lambda_1(k_2^2+\lambda_2^2) , \tag{24}$$

$$D = \{C^2-[(\mathbf{k}_1-\mathbf{k}_2)^2+(\lambda_1+\lambda_2)^2] \times (k_1^2+\lambda_1^2)(k_2^2+\lambda_2^2)\}^{1/2} , \tag{25}$$

and its variations obtained by parametric differentiation. The phases of the square roots of complex numbers are determined by the requirement that the sign of the imaginary part becomes consistent with that of the Green's function.

The differential cross section in the center-of-mass frame is calculated by [13]

$$\frac{d\sigma}{d\Omega} = \frac{\mu_T \mu_P}{4\pi^2} \frac{k_f}{k_i} |T_1+T_2|^2 , \tag{26}$$

and it is converted to the laboratory frame when necessary.

III. RESULTS AND DISCUSSIONS

The three-dimensional integrals of the second-order terms are evaluated directly by a numerical quadrature based on the nine-point Newton-Cotes scheme. The convergence of the integration is carefully checked by supplementing and comparing with the results of the Gauss quadrature and the Romberg formula. The intervals of the integral are divided into pieces, and the number of points is doubled for each piece of intervals iteratively until satisfactory convergence is achieved.

A. $p+H \rightarrow H+p$

In advance of investigating rearrangement collisions of exotic atoms, we show the results of proton-hydrogen collisions, since this process serves as a prototype of vari-

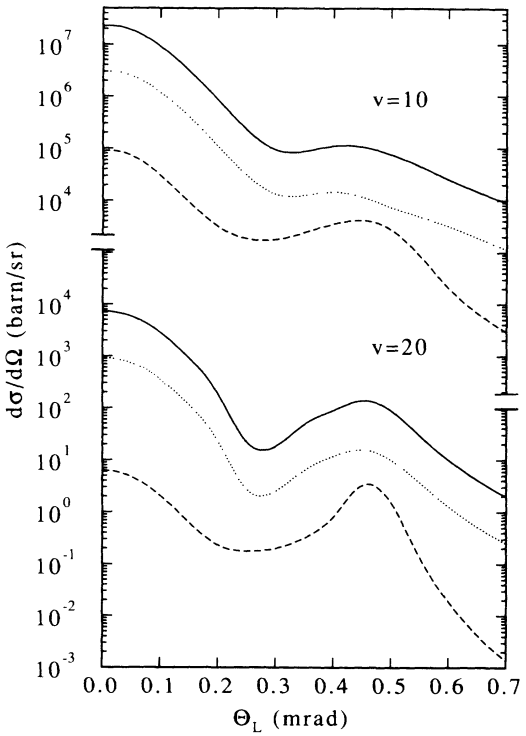

FIG. 1. The second-order Born differential cross sections in the laboratory frame for $p+H \rightarrow H+p$ at $v=10$ a.u. (2.5 MeV, upper three curves) and $v=20$ a.u. (10 MeV, lower three curves). The solid, dotted, and dashed lines are for capture to $1s$, $2s$, and $2p$, respectively.

ous capture processes. No exact calculation of the second-order Born terms has been executed for capture to excited states before. Figure 1 shows the differential cross sections in the laboratory frame at $v=10$ and 20 a.u. (corresponding to the collision energies of 2.5 and 10 MeV, respectively). While the shape of the differential cross section for capture to $2s$ is very similar to that of $1s$ at both energies, the differential cross section for capture to the $2p$ state has a different shape. The difference becomes larger as the collision energy increases. The forward peak decreases faster than the Thomas peak, which is located at 0.47 mrad in the laboratory frame. At $v=20$ a.u., the peak value of $2p$ cross section at the Thomas angle is comparable to the forward peak value.

B. $p+(p\mu^-)\rightarrow(p\mu^-)+p$

Figure 2 gives the differential cross sections in the laboratory frame at $v=10$ and 20 a.u. (2.5 and 10 MeV). Though this process is analogous to the proton-hydrogen collision, there exist some differences owing to the fact that the mass of a muon is 207 times larger than that of an electron. One is the shift of Thomas critical angle to a larger angle of 0.1 rad and another is the smallness of the capture cross section. The geometrical size of the atom $(p\mu^-)$ is about $\frac{1}{207}$ of a hydrogen atom. This makes the total cross section smaller by a factor of $(\frac{1}{207})^2$. The extension of the angular distribution up to larger scattering angles diminishes the absolute value of the differential cross section further. The cross sections approximately obey scaling from the results of proton-hydrogen collisions; the absolute value is reduced by a factor of $(\frac{1}{207})^4$ and the angular distribution is stretched by a factor of 207. The validity of the scaling is mainly due to the fact that both $p+\mathrm{H}$ and $p+(p\mu^-)$ are symmetric for the interchange of the projectile and the target nuclei. The difference of the binding energies between (pe^-) and $(p\mu^-)$ affects the kinematics only a little.

C. $\mu^+ + (p\mu^-)\rightarrow(\mu^+\mu^-)+p$

Figure 3 gives the differential cross sections in the laboratory frame at $v=20$ and 30 a.u. (1.13 and 2.55 MeV). In this process two paths lead to the Thomas double scattering at the same scattering angle of 48° and they interfere analogously to the positronium formation from a hydrogen atom,

$$e^+ + \mathrm{H} \rightarrow \mathrm{Ps} + p \ , \tag{27}$$

in which the critical angle is located at 45°. However, scaling from the data of the positronium formation [10] does not hold well. In the collisions of $\mu^+ + (p\mu^-)$ and $e^+ + \mathrm{H}$, the kinematics is influenced directly by the mass ratio M_c/M_T owing to the asymmetry of the initial and final channels. Two sharp dips were seen at $v=20$ a.u. in

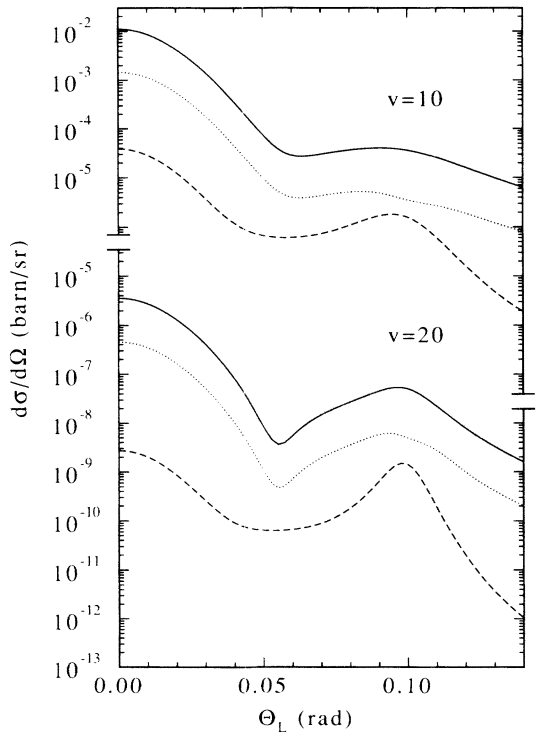

FIG. 2. The second-order Born differential cross sections in the laboratory frame for $p+(p\mu^-)\rightarrow(p\mu^-)+p$ at $v=10$ a.u. (2.5 MeV, upper three curves) and $v=20$ a.u. (10 MeV, lower three curves). The solid, dotted, and dashed lines are for capture to $1s$, $2s$, and $2p$, respectively.

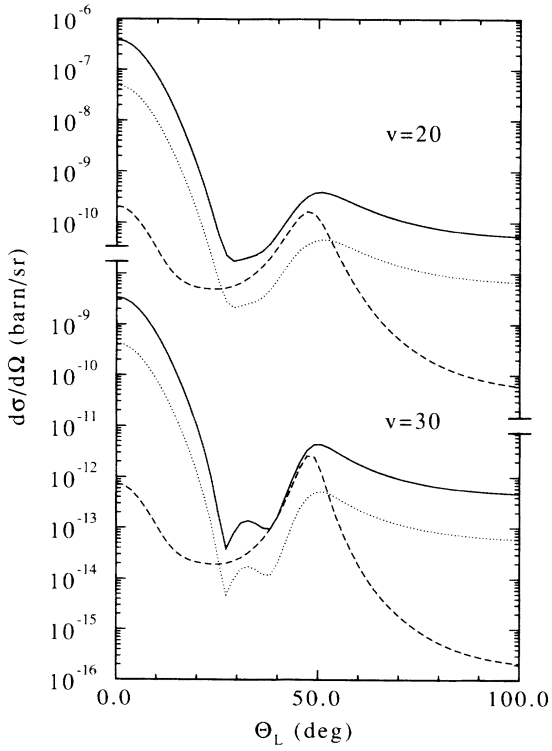

FIG. 3. The second-order Born differential cross sections in the laboratory frame for $\mu^+ + (p\mu^-)\rightarrow(\mu^+\mu^-)+p$ at $v=20$ a.u. (1.13 MeV, upper three curves) and $v=30$ a.u. (2.55 MeV, lower three curves). The solid, dotted, and dashed lines are for capture to $1s$, $2s$, and $2p$, respectively.

the process (27), but, in the present process, we see no dip in the figure at the same velocity. At $v=30$ a.u., two dips exist in the differential cross sections for the capture of $1s$ and $2s$ while the cross section for $2p$ state has still no dip there. As shown in Ref. [10], the dips are not caused by the destructive interference of the two second-order terms but rather by the interference between the first-order terms and the real part of the second-order terms. In fact, the dip angles, 26° and 39°, do not coincide with the Thomas angle of 48°.

D. $e^+ + (e^+e^-) \rightarrow (e^+e^-) + e^+$

This process has a peculiarity that all the three particles have an equal mass. In this kind of process, the quantal and the classical predictions of the Thomas processes disagree. All the three Thomas processes (i)–(iii) give the same critical angle of 180° but the two paths (ii) and (iii) are forbidden in the classical mechanics. In the first mechanism (i), the projectile positron makes a head-on collision with the electron at first. The projectile stops there because of the equality of the masses and the electron instead begins to run with the incident velocity of the projectile. The electron makes a secondary head-on collision with the target positron and stops there to make a bound state with the projectile positron. These two successive head-on collisions result in a backward scattering if it is seen in the center-of-mass frame. This process is really possible, though the probability seems very small. In the second mechanism (ii), the projectile positron makes a zero-angle scattering with the electron at first, and in the second step it makes a head-on collision with the target positron. In the third mechanism (iii), the projectile positron makes a head-on collision with the target positron at first, and in the second step the ejected target positron makes a zero-angle scattering with the electron. The problem is the zero-angle scatterings in these two paths. Zero-angle scatterings occur only at infinite-impact-parameter encounters for Coulomb potentials, and thus they are forbidden for electrons in a bound state. On the other hand, all of the three paths are possible in the quantum mechanics, since they arise from the singularity of the Green's function.

The term (16) can also contribute to the backscattering. This is a second-order correction of the first-order knock-on process. When the masses of the projectile P and the target T are equal, a single head-on collision between these two particles can also induce particle transfer as a first-order process, as shown by Mapleton [16].

Figure 4 shows the differential cross sections at $v=10$ and 20 a.u. (1.36 and 5.44 keV). In this figure we use the center-of-mass frame, which is more convenient to show backscatterings. While all of the curves show the dominance of the backscattering contribution, there is a difference between the shapes of the cross sections of $1s$ and of the excited states. The differential cross sections for the excited states show a dip at $\theta=180°$, but that for $1s$ is smooth there. This is caused by the fact that the first-order knock-on capture is not allowed if the initial and final states have different quantum numbers. In the first-order process, the electron does not participate in the collision process directly. It continues to be in the same state without perceiving the interchange of the center of Coulomb force (positron in this case). The nonzero values of the cross sections of $2s$ and $2p$ at $\theta=180°$ arise only from the second-order contribution. Among the second-order terms, the term (13) gives a much smaller contribution than the other two terms (14) and (15) at variance with the classical prediction. The term (16) gives the largest contribution.

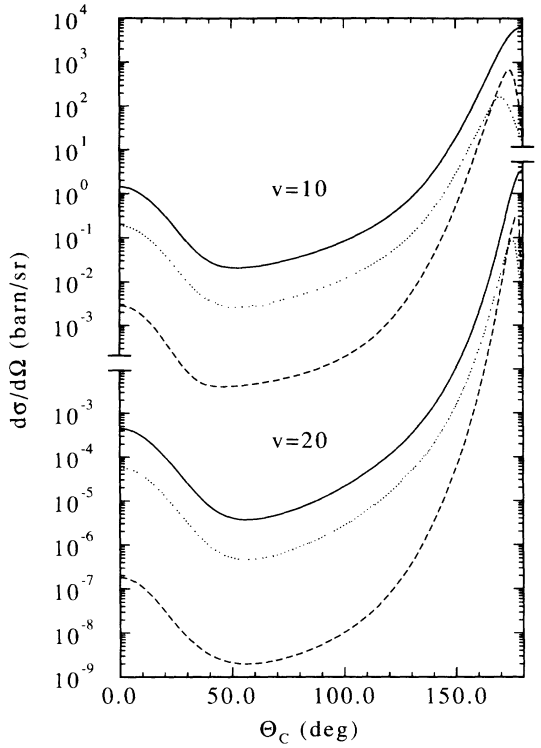

FIG. 4. The second-order Born differential cross sections in the center-of-mass frame for $e^+ + (e^+e^-) \rightarrow (e^+e^-) + e^+$ at $v=10$ a.u. (1.36 keV, upper three curves) and $v=20$ a.u. (5.44 keV, lower three curves). The solid, dotted, and dashed lines are for capture to $1s$, $2s$, and $2p$, respectively.

We show the differential cross section of the first-order Born approximation at $v=10$ a.u. in Fig. 5. The first-order cross sections for the $1s$ and the $2s$ states have a dip at 45°. This dip is caused by the mutual cancellation of the two terms of the first-order T matrix element. p states have three sublevels, and the sum over these sublevels smears out the dip. We see that the contribution of the second-order terms is sizable in the angular range less than 70°.

Though the two positrons are identical particles, we have not antisymmetrized the positron wave function in the present treatment to show the backscatterings more clearly. If the wave function is antisymmetrized properly, the transition amplitude for electron exchange becomes a linear combination of the direct-pickup part calculated in the present study and its counterpart for the interchange of the positrons, the latter of which corresponds to elastic (or excitation for $n=2$ shell) scatterings between a positron and a positronium. Since the position

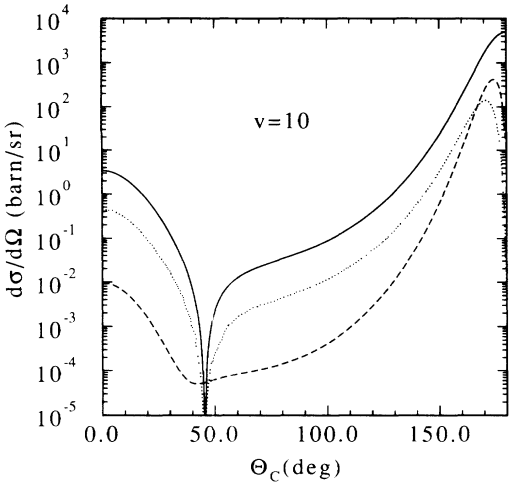

FIG. 5. The first-order Born differential cross sections in the center-of-mass frame for $e^+ + (e^+e^-) \rightarrow (e^+e^-) + e^+$ at $v = 10$ a.u. (1.36 keV). The solid, dotted, and dashed lines are for capture to $1s$, $2s$, and $2p$, respectively.

vector between the atomic system and the ion is measured antiparallelly in these two amplitudes, the forward part of the elastic-scattering amplitude is added to (or subtracted from, depending on the spin symmetry) the backward part of the pickup-scattering amplitude. The peak of the pickup backscatterings may be masked by the sharper peak of the elastic forward scattering.

IV. SUMMARY

We have calculated the second-order Born cross section for exotic-atom formation rigorously without a recourse to any further approximation. The processes can be classified into three types. The first type is analogous to the ordinary electron-capture processes in ion-atom collisions. Only one path is possible for the Thomas double scattering. The second one is analogous to positronium formation in positron-atom collisions. Two different paths are contributing to the Thomas process, and they interfere. The third one is the case in which all three particles have equal masses. The two second-order terms (ii) and (iii) that have no classical analogue are contributing significantly to the backscatterings. Unfortunately, no experimental data are available at present for the processes studied in this paper. The authors hope that the present results may help for planning a new experiment on exotic-atom formations.

[1] L. H. Thomas, Proc. R. Soc. London **114**, 561 (1927).
[2] R. M. Drisko, Ph.D. thesis, Carnegie Institute of Technology, 1955.
[3] Nonperturbative studies of the Thomas process have been carried out recently by the coupled-channel method and by the classical trajectory Monte Carlo method: N. Toshima and J. Eichler, Phys. Rev. Lett. **66**, 1050 (1991); Phys. Rev. A **46**, 2564 (1992); N. Toshima, *ibid.* **42**, 5739 (1990); **45**, 2663 (1992).
[4] R. Shakeshaft and J. M. Wadehra, Phys. Rev. A **22**, 968 (1980); J. H. McGuire, N. C. Sil, and N. C. Deb, *ibid.* **34**, 685 (1986).
[5] D. R. Bates, C. J. Cook, and F. J. Smith, Proc. Phys. Soc. London **83**, 49 (1964).
[6] K. Dettman and G. Leibfried, Z. Phys. **218**, 1 (1969).
[7] P. J. Kramer, Phys. Rev. A **6**, 2125 (1972); N. Toshima and A. Igarashi, *ibid.* **45**, 6313 (1992).
[8] P. R. Simony and J. H. McGuire, J. Phys. B **14**, L737 (1981); J. E. Miraglia, R. D. Piacentini, R. D. Rivarola, and A. Salin, *ibid.* **14**, L197 (1981).
[9] Dž. Belkić, Europhys. Lett. **7**, 323 (1988); Phys. Rev. A **43**, 4751 (1991); D. P. Dewangan and B. H. Bransden, J. Phys. B **21**, L353 (1988); F. Decker and J. Eichler, *ibid.* **22**, L95 (1989); **22**, 3023 (1989).
[10] J. R. Oppenheimer, Phys. Rev. **31**, 349 (1928); H. C. Brinkman and H. A. Kramers, Proc. K. Ned. Akad. Wet. **33**, 973 (1930).
[11] R. Schakeshaft and L. Spruch, Rev. Mod. Phys. **51**, 369 (1979).
[12] A. Igarashi and N. Toshima, Phys. Rev. A **46**, 1159 (1992).
[13] M. R. C. McDowell and J. P. Coleman, *Introduction to the Theory of Ion-Atom Collisions* (North-Holland, Amsterdam, 1970).
[14] J. D. Jackson and H. Schiff, Phys. Rev. **89**, 359 (1953).
[15] R. R. Lewis, Jr., Phys. Rev. **102**, 537 (1956).
[16] R. A. Mapleton, Proc. Phys. Soc. London **83**, 895 (1964).